Local auxin biosynthesis regulation by PLETHORA transcription factors controls phyllotaxis in *Arabidopsis*

Violaine Pinon[a,1], Kalika Prasad[a,b], Stephen P. Grigg[a,1], Gabino F. Sanchez-Perez[a,c], and Ben Scheres[a,1,2]

[a]Molecular Genetics, Department of Biology, Faculty of Science, Utrecht University, 3584 CH Utrecht, The Netherlands; [b]School of Biology, Indian Institute of Science Education and Research, Kerala 695016, India; and [c]Plant Research International, Wageningen University, 6708 PB, Wageningen, The Netherlands

Edited by Mark Estelle, University of California at San Diego, La Jolla, CA, and approved December 5, 2012 (received for review August 3, 2012)

Lateral organ distribution at the shoot apical meristem defines specific and robust phyllotaxis patterns that have intrigued biologists and mathematicians for centuries. *In silico* studies have revealed that this self-organizing process can be recapitulated by modeling the polar transport of the phytohormone auxin. Phyllotactic patterns change between species and developmental stages, but the processes behind these variations have remained unknown. Here we use regional complementation experiments to reveal that phyllotactic switches in *Arabidopsis* shoots can be mediated by PLETHORA-dependent control of local auxin biosynthesis.

pattern formation | plant

In higher plants lateral organs are generated at the plant apex by shoot apical meristems (SAMs), which maintain self-renewing stem cell populations and allocate daughters to organ primordia. SAM organization can be classified into three functionally and spatially distinct zones: a central zone (CZ) containing slowly dividing stem cells at the apex and cells forming the organizing center below the stem cell niche, a peripheral zone (PZ) characterized by rapidly dividing cells that can be incorporated into organ primordia, and a rib zone (RZ) underlying the CZ and the PZ producing cells that form the bulk of the stem (1). In *Arabidopsis* stem cell homeostasis is regulated by a signaling mechanism of which the homeodomain protein WUSCHEL (WUS) and the secreted glycopeptide CLAVATA3 (CLV3) are key components (2–4). The class I *Knotted*-like homeobox (KNOX) gene *SHOOTMERISTEMLESS* (*STM*) maintains meristem integrity by preventing cell differentiation (5–7).

The distribution of lateral organs along the stem, known as phyllotaxis, follows regular patterns that can be described mathematically (8, 9). One commonly observed pattern is the spiral phyllotaxis characterized by the "golden angle," where successive organs form angles of about 137°. When two organs are initiated simultaneously as an opposite pair, shifted 90° with respect to the previous pair, they form a "decussate" pattern. "Distichous" phyllotaxis, as observed in maize and rice, is characterized by organs initiating sequentially at 180° angles.

Organogenesis at the SAM is triggered by the accumulation of the phytohormone auxin (10). Based on the expression patterns of the auxin biosynthesis genes *YUCCA1* (*YUC1*), *YUC2*, *YUC4*, *YUC6*, and *TRYPTOPHAN AMINOTRANSFERASE OF ARABIDOPSIS1* (*TAA1)*, auxin is thought to be produced throughout the meristem dome (11–13) and redistributed toward incipient primordia mainly via the active efflux transporter PIN1 (10, 14–16). In agreement with this idea, influx and efflux auxin transporters are required for correct organ positioning (15, 17, 18). Early experiments demonstrated that the position of new primordia depends on the position of older ones (19), leading to a lateral inhibition model of phyllotaxis wherein each organ primordium acts as an auxin sink, thus depleting auxin locally and creating an inhibitory field where no other organ can initiate (15). Using computational models, it has been predicted that a feedback from auxin accumulation or flux to *PIN1* expression or polarity can explain patterns of phyllotaxis seen in nature (20–22).

Recently we reported that the *plethora3, plt5, plt7* triple mutant is defective in establishing spiral phyllotaxis and can adopt a metastable distichous pattern on several consecutive nodes (18). Contrasting this phenotype, many other phyllotaxis mutants display random patterns of organ formation. Moreover, previously described defects in phyllotaxis often represent one aspect of a pleiotropic phenotype, thus complicating the distinction between direct and indirect effects. The three partially redundant *PLETHORA* genes *PLT3*, *PLT5*, and *PLT7* encode AP2 domain transcription factors expressed in overlapping domains in the center of the meristem, and in organ primordia at different stages of development (18, 23). Here we dissect which domain of *PLT* expression is required for spiral phyllotaxis and use this information to shed light on the molecular mechanisms controlling phyllotactic stability. Whereas the three *PLT* genes are required to maintain high levels of *PIN1* expression at the periphery of the meristem (18), our study demonstrates that modulation of local auxin production in the central region of the SAM underlies phyllotactic transitions.

Results

PLETHORA Activity in the Meristem Center Is Necessary and Sufficient for Spiral Phyllotaxis. Although PLT activity is required for acute *PIN1* up-regulation at sites of incipient primordia in the PZ, the greatest overlapping expression of the relevant *PLT* genes resides at the CZ (18). We therefore asked where PLT transcription factors are required to control spiral phyllotaxis by conducting domain-specific complementation of *plt3plt5plt7* triple mutants. Variations in frequencies of the two angle attractors 137° and 180° were seen frequently in *plt3plt5plt7* (Figs. 1 *B* and *F* and 2*B Upper*). However, the triple mutant consistently showed a decreased stability of the spiral pattern associated with an increased stability of the distichous pattern (Figs. 1 *B* and *F* and 2*B Lower*). Based on these observations we assessed the *plt3plt5plt7* phyllotaxis phenotype by analyzing both the distribution of angles (Fig. 1 *Upper*) and patterns (Fig. 1 *Lower*). Spiral phyllotaxis was completely restored when *PLT* genes were expressed throughout the meristem (CZ and PZ), excluding organ primordia, under the *STM* promoter (Fig. 1 *A–C* and Figs. S1 *A*, *C*, and *D* and S2*A*) (5). Expression of *PLT* in the stem cells of the CZ using the *CLV3* promoter also fully complemented *plt3plt5plt7* phyllotactic defect (Fig. 1 *E–G* and Figs. S1 *C* and *D* and S2*D*) (2). Partial complementation was observed using the *WUS* promoter, which is active in the cells of the organizing center (Fig. 1 *E*, *F*, and *H* and Figs. S1 *C* and *D* and S2*E*) (24). Surprisingly, driving expression of *PLT* genes from the organ-specific *AINTEGUMENTA* (*ANT*) and *FILAMENTOUS FLOWER* (*FIL*) promoters failed to complement the *plt3plt5plt7* mutant phenotype (Fig. 1 *A*, *B*, and *D* and Figs. S1 *B* and *C* and S2 *B* and *C*) (25, 26). Cells in organ primordia of these noncomplementing *pANT::PLT5:VENUS* and *pFIL::PLT5:VENUS plt3plt5plt7* lines showed similar (or higher)

Author contributions: V.P. and B.S. designed research; V.P. and S.P.G. performed research; K.P., S.P.G., and G.F.S.-P. contributed new reagents/analytic tools; V.P. and S.P.G. analyzed data; and V.P. wrote the paper.

The authors declare no conflict of interest.

This article is a PNAS Direct Submission.

[1]Present address: Plant Developmental Biology, Plant Sciences Group, Wageningen University, 6708 PB Wageningen, The Netherlands.

[2]To whom correspondence should be addressed. E-mail: ben.scheres@wur.nl.

This article contains supporting information online at www.pnas.org/lookup/suppl/doi:10.1073/pnas.1213497110/-/DCSupplemental.

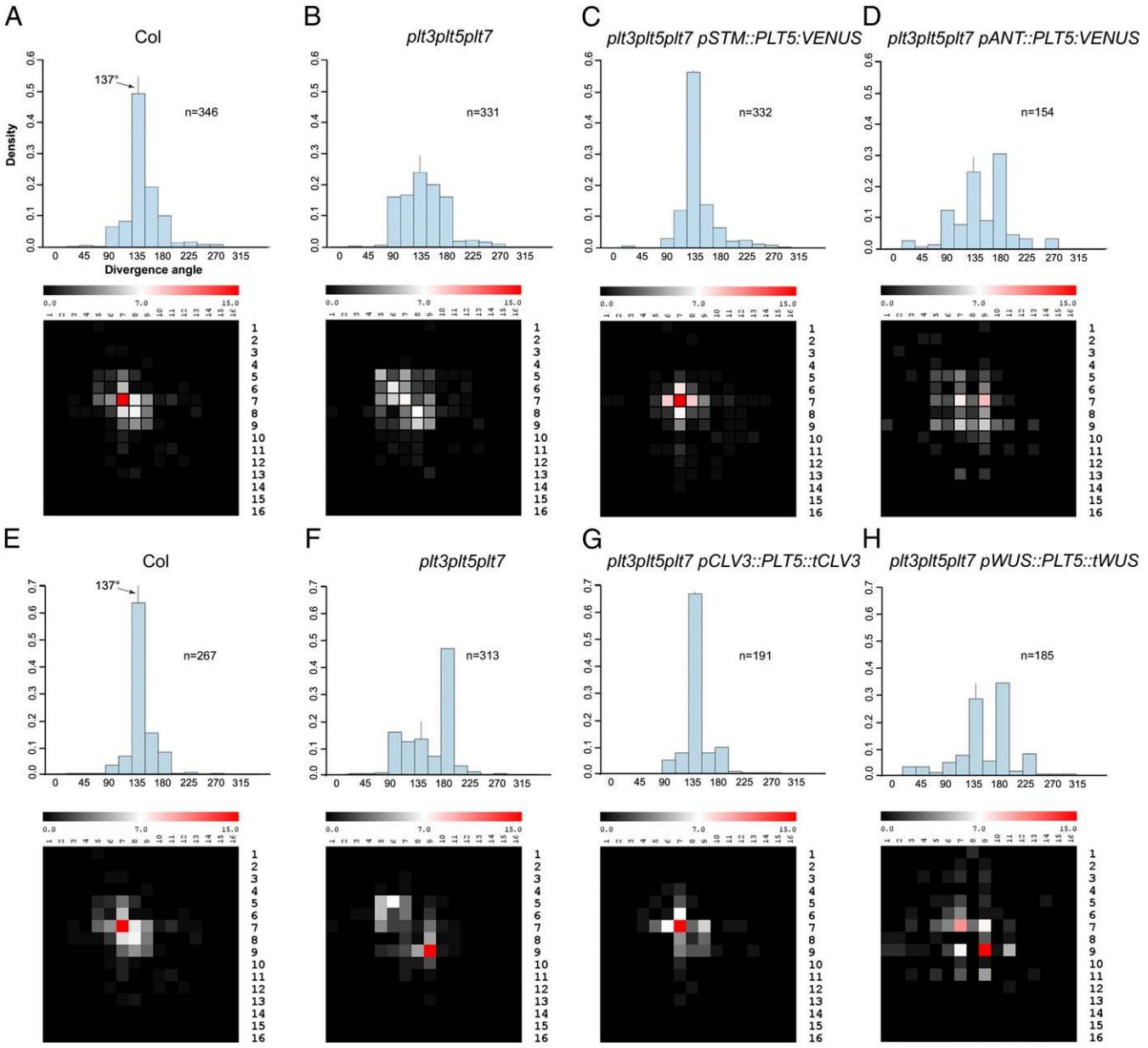

Fig. 1. Expression of *PLT5* in the SAM center is sufficient to complement the *plt3plt5plt7* phyllotaxis defect. (*A*) Silique divergence angle distribution in wild-type Col inflorescences; angle classes are defined by their midpoint (*Upper*). In a two-entry map, the distribution of divergence angle patterns between three successive siliques in Col is shown (*Lower*). This representation shows for each angle category (*x* axis) the occurrence of the angle class for the next internode (*y* axis), represented by color intensity. The angles have been divided into 16 classes separated by 22.5° (axes *x* and *y*). The angle class 7 comprises the "golden angle" 137°, and class 9 includes the angle 180°. In Col, when two siliques are separated by 137° (angle category 7 on the *x* axis), the highest frequency for the third consecutive silique falls in category 7 (*y* axis), showing that successive organs preferentially adopt a spiral pattern. Silique divergence angle distribution in *plt3plt5plt7* mutant (*B Upper*), *plt3plt5plt7 pSTM::PLT5:VENUS* (*C Upper*), and *plt3plt5plt7 pANT::PLT5:VENUS* (*D Upper*). Corresponding lower panels display the distribution of patterns in successive silique divergence angles from the same experiment. Silique divergence angle distribution (*Upper*) and corresponding silique pattern distribution (*Lower*) in Col (*E*), *plt3plt5plt7* (*F*), *plt3plt5plt7 pCLV3::PLT5::tCLV3* (*G*), and *plt3plt5plt7 pWUS::PLT5::tWUS* (*H*). *A–D* and *E–H* represent two experiments. n, number of divergent angles.

fluorescence levels compared with those in complementing *pPLT5::PLT5:VENUS plt3plt5plt7* lines (Fig. S3 *A–G*); therefore, lack of complementation was not due to low expression level. Because we never observed accumulation of those proteins outside their expected domains, we conclude that PLT transcription factors act in the center of the meristem to control organ patterning, rather than in organ primordia, as was previously postulated (18).

PLT-Dependent *PIN1* Expression at the Meristem Does Not Directly Contribute to Phyllotaxis. *PIN1* auxin efflux carrier is expressed in the outermost layer of cells (L1) in the meristem, both in organ primordia and in the center of the meristem (15). According to simulation of polar auxin transport on templates with realistic PIN distributions (27) and examination of the auxin input signaling marker DII (28, 29), auxin accumulates in the CZ of the SAM, suggesting a role for the meristem center in auxin distribution. Therefore, PLT activity in the center of the meristem might also be involved in the regulation of *PIN1* expression, as in organ primordia (18). To investigate whether PLT regulates phyllotaxis through PIN1 levels in the SAM, we expressed *PIN1:GFP* under *CLV3* and *STM* promoters in *plt3plt5plt7* mutants. Neither construct was sufficient to restore spiral phyllotaxis in

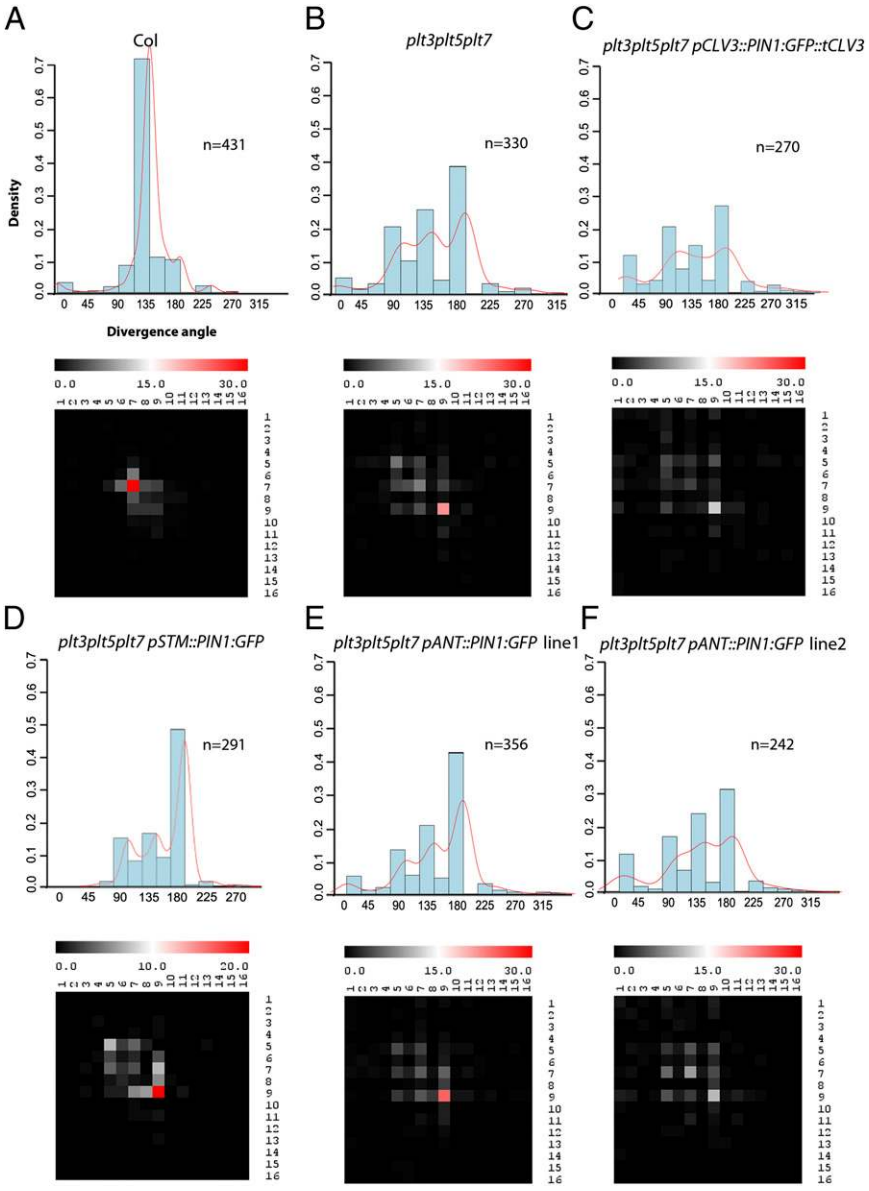

Fig. 2. Expression of PIN1:GFP in the center of the meristem and in organ primordia does not complement *plt3plt5plt7* phyllotaxis defect. Silique divergence angle distribution (*Upper*) and corresponding silique divergence angle pattern distribution (*Lower*) in Col (*A*), *plt3plt5plt7* (*B*), *plt3plt5plt7 pCLV3::PIN1:GFP::tCLV3* (*C*), *plt3plt5plt7 pSTM::PIN1:GFP* (*D*), *plt3plt5plt7 pANT::PIN1:GFP line1* (*E*), and *plt3plt5plt7 pANT::PIN1:GFP line2* (*F*). n, number of divergence angles.

plt3plt5plt7 (Fig. 2 *A–D* and Fig. S4 *A* and *B*). We concluded that *PLT* genes do not promote spiral phyllotaxis by positively regulating *PIN1* expression in the center of the meristem. We have previously shown that increasing the amount of PIN1 in organ primordia can partly complement the *plt3plt5plt7* phyllotaxis defect (18). Intriguingly, we now observe that PLT transcription factors appear to regulate organ patterning from the meristem center, rather than from organ primordia. This result suggested to us that *PIN1* down-regulation in *plt3plt5plt7* might not be the direct cause of the phyllotaxis phenotype. In Prasad et al. (18), the angles of isolated internodes were categorized into six classes between 0° and 180°, and the resulting distribution showed that pANT::PIN1:GFP in *plt3plt5pt7* confers a relative decrease of about 50% of the 180° angle category and an increase of about 18% of the category including the "golden angle." A range of additional angles was also observed. We decided to reassess the extent to which the angle and pattern distributions are complemented in *plt3plt5plt7* phenotype with a more detailed analysis in independent T2 lines expressing pANT::PIN1:GFP in *plt3plt5plt7* with expression levels of PIN1:GFP similar to pPIN1::PIN1:GFP in wild-type background (Fig. 2 *A*, *B*, *E*, and *F* and Fig. S5 *A* and *B*). Although we again observed variations in frequencies of the 137° and 180° angle categories (Fig. 2 *E* and *F Upper*), the distichous pattern was more stable than the spiral phyllotaxis (Fig. 2 *E* and *F Lower*). In conclusion, whereas expression of PIN1 can be affected in *plt3plt5plt7*, PIN1 reexpression in *plt3plt5plt7* organ primordia is not sufficient to fully rescue the mutant. All together our data indicate that *PIN1* transcriptional regulation by PLT at the SAM does not directly control phyllotaxis.

Auxin Abundance Changes in the Center of the Meristem Can Promote Phyllotactic Transitions. Previously published data suggest that *PLT* genes control auxin abundance in the root meristem (30). A similar scenario could then occur at the SAM to control organ patterning. Auxin abundance depends on polar auxin transport and auxin biosynthesis. We have demonstrated that PLT proteins exert their control on phyllotaxis from the SAM center in a process that does not involve *PIN1* transcriptional regulation. Therefore, we asked whether PLT proteins constitute upstream components modulating auxin biosynthesis in the SAM. *YUCCA1* (*YUC1*) and *YUC4*, which encode flavin-containing monooxygenases involved in a rate-limiting step of auxin biosynthesis (31, 32), are expressed both in the center of the meristem and in organ primordia, overlapping with *PLT* expression domains (11).

The expression levels of both *YUC1* and *YUC4* were reduced in *plt3plt5plt7* mutant shoot apices (Fig. 3 *A* and *B*), suggesting that PLT proteins stimulate *YUC* expression. Furthermore, we observed increased *YUC4* transcript levels after 2 and 4 h of PLT5 induction, using an inducible PLT5:GR construct, even when the translational machinery was inhibited by cycloheximide (CHX) (Fig. 3*C*), indicating that auxin biosynthesis genes are rapidly and possibly directly activated by PLT activity. If decreased auxin production at the SAM is responsible for the phyllotaxis defect observed in *plt3plt5plt7*, then low-auxin mutants might display similar phenotypes. We therefore measured phyllotactic patterns among the progeny of *yuc1*/+ *yuc4* plants, because *yuc1yuc4* double mutants generate no or very few lateral organs (11). We observed a shift from spiral phyllotaxis to a metastable distichous pattern in this population (Fig. 3 *D*–*F*), similar to the *plt3plt5plt7* phenotype. This result suggests that PLT proteins control phyllotaxis via YUC-mediated control of auxin biosynthesis in the SAM. To confirm this hypothesis we restored *YUC4* expression in *plt3plt5plt7* using the *STM* and *FIL* promoters. When *YUC4* was expressed under the *STM* promoter, the phyllotaxis of the mutant was fully rescued to a spiral pattern (Fig. 3 *D*, *E*, and *G* and Fig. S6 *A* and *C*–*F*), whereas expressing *YUC4* in organ primordia from the *FIL* promoter did not complement the organ patterning defect of *plt3plt5plt7* (Fig. 3 *D*, *E*, and *H* and Fig. S6 *B* and *G*). Therefore, the phyllotactic shifts in *plt3plt5plt7* mutants likely reflect a failure to synthesize auxin in the SAM center rather than in organ primordia, highlighting the importance of SAM-derived auxin in phyllotaxis. We conclude that PLT proteins control the abundance of auxin in the SAM by regulating expression of *YUC1* and *YUC4*.

Auxin Signaling Is Reduced in *plt3plt5plt7* Mutant Shoot Meristems. Our data show that PLT proteins promote auxin biosynthesis in the center of the SAM to control organ position, rather than in the incipient primordia, which likely act as auxin sinks. In agreement with this idea, PIN1 accumulation, which positively responds to auxin levels, is reduced in organ primordia in *plt3plt5plt7* mutants (Fig. 4 *B* and *D*) (18). To infer the auxin levels in floral primordia we analyzed expression of the DR5::nuc VENUS auxin activity reporter together with pPIN1::PIN1:GFP in *plt3plt5plt7* mutant SAMs (Fig. 4). In wild type, sites of DR5:: nucVENUS expression correlate with pPIN1::PIN1:GFP up-regulation at the PZ of the meristem (Fig. 4 *A* and *B*) (33). The number of cells per early primordium expressing DR5 in *plt3plt5plt7* was approximately half of the number in wild type (wild-type Col: 14.8, $n = 36$, SE = 1.07; *plt3plt5plt7*: 7.1, $n = 61$, SE = 0.65). Reduced DR5::nucVENUS expression was observed in primordia that did show obvious up-regulation of pPIN1:: PIN1:GFP (Fig. 4*C*) as well as in those that did not (Fig. 4*D*). This observation indicates that low DR5::nucVENUS in primordia is not caused by the absence of PIN1 up-regulation at those sites, but rather by low auxin levels in the SAM. The correlation between reduced CZ auxin biosynthesis and decreased auxin response in incipient primordia supports the conclusion that auxin synthesized in the center of the meristem is essential for the control of phyllotaxis.

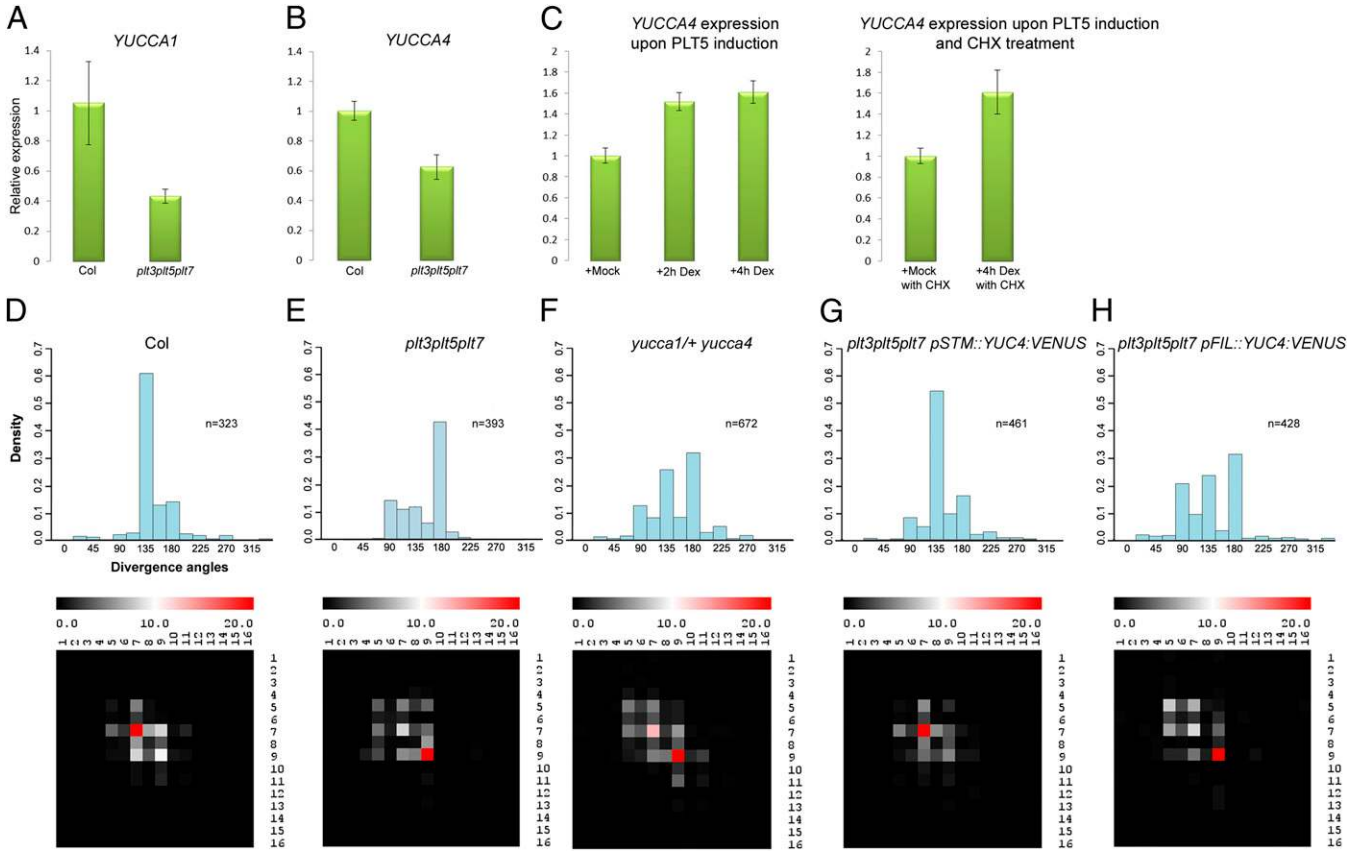

Fig. 3. *PLT* genes regulate phyllotaxis through the transcription of the auxin biosynthetic genes *YUC1* and *YUC4*. *YUC1* (*A*) and *YUC4* (*B*) expression levels measured by quantitative RT-PCR in Col and *plt3plt5plt7* dissected 10 d-old (do) shoot apices. (*C*) *YUC4* expression level after 2 and 4 h of PLT5 induction by DEX (*Left*) and after 4 h of DEX and CHX treatments (*Right*). Error bars represent the SE from three independent experiments. Distribution of silique divergence angles (*Upper*) and corresponding silique divergence angle pattern distribution (*Lower*) in Col (*D*), *plt3plt5plt7* (*E*), *yuc1*/+*yuc4* (*F*), *plt3plt5plt7 pSTM::YUC4:VENUS* (*G*), and *plt3plt5plt7 pFIL::YUC4:VENUS* (*H*). n, number of divergence angles.

Discussion

The distribution of auxin through the efflux carrier PIN1 is key to the establishement of stable phyllotactic patterns (20–22, 27). However, it is still unclear whether the transported auxin is synthesized in the SAM (21, 27) or is imported from lateral developing organs through epidermal PIN1 (15, 33, 34). Here we propose that local auxin biosynthesis in the center of the meristem, under the control of PLT transcription factors, stabilizes spiral phyllotaxis. One plausible scenario is that PLT proteins regulate phyllotaxis by ensuring sufficient production of auxin in the SAM to initiate organs in a spiral pattern. In *plt3plt5plt7* mutants, auxin thresholds for organ initiation are not reached at the correct position because of insufficient auxin levels in the SAM. When *PLT* or *YUC4* genes are expressed throughout the SAM from the *STM* promoter in *plt3plt5plt7*, auxin levels in the SAM increase and a wild-type inhibitory field is restored. In contrast, *ANT* and *FIL* promoters, which are specifically active in organ primordia after patterning process, can cause the auxin produced to be sequestered in the developing organ, where it remains unavailable to the meristem and thus cannot contribute to organ patterning.

Until now mathematical models of auxin-dependent processes such as phyllotaxis have mainly focused on polar auxin transport. Our work clearly shows that the quantity and the specific localization of auxin production in the SAM center can orchestrate organ distribution at the shoot apex. It will be interesting to implement local auxin biosynthesis into diverse *in silico* phyllotaxis models and probe to what extent altering this variable can provoke stable transitions. Reminiscent of *plt3plt5plt7* mutants, transient distichous patterns emerge in mathematical models of phyllotaxis implementing noise on organ initiation threshold either by modifying the sensitivity of the cell response or by inducing fluctuations in auxin levels (35). In the light of this model we propose that PLT-induced local auxin biosynthesis in the meristem reduces noise in organ patterning.

Phyllotaxis is also known to depend on meristem size (36, 37). The phytohormone cytokinin (CK) is an important factor for shoot meristem maintenance and organ positioning (37–40). Auxin has been implicated in the regulation of *CLV3* through CK signaling, suggesting that auxin homeostasis in the SAM is important to control stem cell fate (40). Auxin levels in the SAM center depend on auxin biosynthesis, which we showed is dependent on PLT transcription factors, and is also likely affected by auxin conjugation, degradation, and its polarized distribution in the apex. Our work shows that PLT-dependent regulation of auxin biosynthesis in the meristem center controls organ patterning. If auxin levels in the SAM center also regulate the size of the stem cell niche, future investigations should reveal whether PLT-mediated auxin biosynthesis coordinates stem cell maintenance and organ patterning.

Materials and Methods

Plant Material and Growth Conditions. The *plt3-2, plt5-2, plt7-1* triple mutant has been described previously (18). The mutant combination *yuc1/+, yuc4-1* was obtained from Yunde Zhao (San Diego, CA) (11). *STM* promoter encompasses a 5-kb upstream fragment (41) amplified with the primers pSTM_1R4_F and pSTM_1R4_R displayed in Table S1. *CLV3* promoter requires a 1.5-kb fragment upstream of the start codon and a 1.2-kb terminator fragment downstream of the stop codon (42). Both fragments were amplified using, respectively, pCLV3_1R4_F and pCLV3_1R4_R primer pair and tCLV3_2R3_F and tCLV3_2R3_R primer pair (Table S1). *WUS* promoter contains a fragment of 1.5 kb upstream of the start codon amplified with pWUS_1R4_F and pWUS_1R4_R primers (Table S1) and a terminator fragment of 3 kb downstream of the stop codon amplified with tWUS_2R3_F and tWUS_2R3_R primers (Table S1) (43). *FIL* promoter comprises 2.9 kb upstream of the *FIL* ATG, amplified using pFIL_1R4_F and pFIL_1R4_R (Table S1). The *ANT* promoter was described previously (18). Genomic sequences of *PLT3*, *PLT5*, and *PLT7,* PIN1:GFP protein fusion, and the inducible *35S::PLT5::GR* construct were described in ref. 18. *YUC4* cDNA, including the start codon but excluding the stop codon, was amplified from Col-0 cDNA with YUC4_221_F and YUC4_221_R primers (Table S1). All of the constructs were generated with the MultiSite Gateway recombination cloning system into pCAMBIA1300 plasmid, transferred to

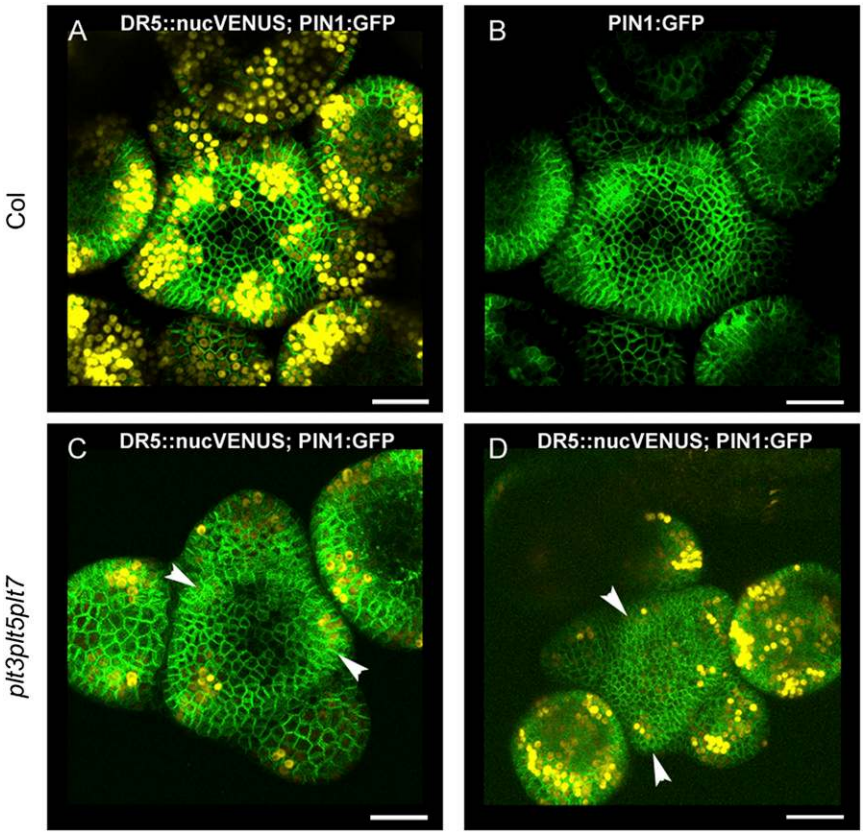

Fig. 4. Auxin signaling is reduced in *plt3plt5plt7* SAM mutants. (*A*) Three-dimensional maximal intensity confocal projection of Col inflorescence meristem expressing DR5::nuclVENUS and pPIN1::PIN1:GFP. (*B*) Same inflorescence as in *A* displaying solely pPIN1::PIN1:GFP to visualize its up-regulation at sites of DR5 expression. (*C–D*) Three-dimensional maximal intensity confocal projection of *plt3plt5plt7* inflorescence meristems expressing DR5::nucVENUS and pPIN1::PIN1:GFP. White arrowheads in *C* show primordia with low DR5 signal despite pPIN1::PIN1::GFP up-regulation. In *D* the arrowheads indicate primordia with DR5 expression and no apparent pPIN1::PIN1:GFP up-regulation. (Scale bars, 20 μm.)

agrobacterium strain C58, and used to produce transgenic plants by floral dipping. Plants were grown either directly on soil or transferred from Murashige and Skoog (MS) medium in long-day conditions of 16 h of light, 22 °C. For each complementation experiment the tested lines were grown along with Col and *plt3plt5plt7* plants to compare plants grown under identical conditions.

Confocal Microscopy. Inflorescence meristems were examined using an upright LSM-710 laser scanning confocal microscope (Carl Zeiss). Single optical sections and 3D projections of the fluorescent signals at the shoot apex were obtained with the ZEN software (Carl Zeiss). Plants were first grown on soil until bolting, then the inflorescence meristems were dissected and immobilized in a thin layer of agarose in a Petri dish as described previously (44).

Dexamethasone Inductions. The *35S::PLT5::GR* seedlings were germinated and grown on MS medium for 10 d. The seedlings were induced for 2 and 4 h in liquid MS medium supplemented with 20 μM dexamethasone (DEX) (Sigma) and harvested for RNA extraction. Mock treatment was carried out using the same medium supplemented with an equal volume of ethanol that was used to dissolve DEX. In the case of CHX treatments, the MS medium was supplemented first with 10 μM of CHX for 15 min and then DEX was added to the medium for the induction.

Measurements of Silique Divergence Angles. Angles separating successive siliques on the main plant inflorescence were estimated using a 360° protractor divided into 16 categories of 22.5° each, with 0° the midpoint of category 1, 137° the midpoint of category 7, and 180° the midpoint of category 9. Inflorescences characterized with counterclockwise spiral were transformed to clockwise as described previously in ref. 18. Two-dimensional histograms displaying the distribution of patterns in successive silique divergence angles were plotted as heat maps using MultiExperiment Viewer (18).

Quantitative Reverse Transcription PCR. Seedlings were grown for 10 d on MS medium and the shoot apices were dissected by cutting out the hypocotyls, cotyledons, and young leaves. Total RNA was extracted with TRIzol reagent (Invitrogen) and purified on-column using a Spectrum Plant Total RNA kit (Sigma Life Science). cDNA synthesis, following DNase treatment, was performed using SuperScriptIII (Invitrogen). All samples were measured on technical triplicates on three biological replicates. The quantitative RT-PCR was performed by using 10 μM of gene-specific primers and *Power SYBR* Green (Applied Biosystems) in an ABI Prism 7000 system. Quantification of gene expression was carried out using the method of Livak and Schmittgen. Results were normalized to that of *ACTIN2*.

Quantification of DR5::YFP Expression. Plants expressing pPIN1::PIN1:GFP and DR5::nucVENUS (33) were scanned by confocal microscopy. Single optical sections and maximum intensity projections were analyzed using ZEN software. Primordia forming a visible protrusion from the SAM flank, and all older primordia, were excluded from scoring. By monitoring individual optical sections, clusters of cells in the PZ showing strong nuclear YFP signal were considered a young primordium, and the number of YFP-positive cells in the L1 cell layer for each young primordium was counted.

ACKNOWLEDGMENTS. V.P. was supported by the European Research and Technology Network (EUR RTN) network Signals and Regulatory Networks in Early Plant Embryogenesis (SIREN) and by European Union Marie Curie Intra-European Fellowship (IEF), S.P.G. was supported by European Union Marie Curie IEF and by the Netherlands Institute of Regenerative Medicine Consortium, G.F.S.-P. was supported by the Conservation Breeding Specialist Group/Netherlands Consortium for Systems Biology program, and B.S. was supported by Netherlands Organization for Scientific Research Spinoza and Systems Biology to Understand Plant Architecture, European Research Council advanced investigator grants.

1. Steeves TA, Sussex IM (1989) *Patterns in Plant Development* (Cambridge Univ Press, New York).
2. Brand U, Fletcher JC, Hobe M, Meyerowitz EM, Simon R (2000) Dependence of stem cell fate in Arabidopsis on a feedback loop regulated by CLV3 activity. *Science* 289(5479):617–619.
3. Lenhard M, Laux T (2003) Stem cell homeostasis in the Arabidopsis shoot meristem is regulated by intercellular movement of CLAVATA3 and its sequestration by CLAVATA1. *Development* 130(14):3163–3173.
4. Ohyama K, Shinohara H, Ogawa-Ohnishi M, Matsubayashi Y (2009) A glycopeptide regulating stem cell fate in Arabidopsis thaliana. *Nat Chem Biol* 5(8):578–580.
5. Long JA, Moan EI, Medford JI, Barton MK (1996) A member of the KNOTTED class of homeodomain proteins encoded by the STM gene of Arabidopsis. *Nature* 379(6560):66–69.
6. Muehlbauer GJ, Fowler JE, Freeling M (1997) Sectors expressing the homeobox gene liguleless3 implicate a time-dependent mechanism for cell fate acquisition along the proximal-distal axis of the maize leaf. *Development* 124(24):5097–5106.
7. Smith LG, Greene B, Veit B, Hake S (1992) A dominant mutation in the maize homeobox gene, Knotted-1, causes its ectopic expression in leaf cells with altered fates. *Development* 116(1):21–30.
8. Douady S, Couder Y (1992) Phyllotaxis as a physical self-organized growth process. *Phys Rev Lett* 68(13):2098–2101.
9. Kuhlemeier C (2007) Phyllotaxis. *Trends Plant Sci* 12(4):143–150.
10. Reinhardt D, Mandel T, Kuhlemeier C (2000) Auxin regulates the initiation and radial position of plant lateral organs. *Plant Cell* 12(4):507–518.
11. Cheng Y, Dai X, Zhao Y (2006) Auxin biosynthesis by the YUCCA flavin monooxygenases controls the formation of floral organs and vascular tissues in Arabidopsis. *Genes Dev* 20(13):1790–1799.
12. Stepanova AN, et al. (2008) TAA1-mediated auxin biosynthesis is essential for hormone crosstalk and plant development. *Cell* 133(1):177–191.
13. Yoshida S, Mandel T, Kuhlemeier C (2011) Stem cell activation by light guides plant organogenesis. *Genes Dev* 25(13):1439–1450.
14. Gälweiler L, et al. (1998) Regulation of polar auxin transport by AtPIN1 in Arabidopsis vascular tissue. *Science* 282(5397):2226–2230.
15. Reinhardt D, et al. (2003) Regulation of phyllotaxis by polar auxin transport. *Nature* 426(6964):255–260.
16. Benková E, et al. (2003) Local, efflux-dependent auxin gradients as a common module for plant organ formation. *Cell* 115(5):591–602.
17. Bainbridge K, et al. (2008) Auxin influx carriers stabilize phyllotactic patterning. *Genes Dev* 22(6):810–823.
18. Prasad K, et al. (2011) Arabidopsis PLETHORA transcription factors control phyllotaxis. *Curr Biol* 21(13):1123–1128.
19. Snow M, Snow RS (1932) Experiments on phyllotaxis. *Philos Trans R Soc Lond B Biol Sci* 221:1–43.
20. Jönsson H, Heisler MG, Shapiro BE, Meyerowitz EM, Mjolsness E (2006) An auxin-driven polarized transport model for phyllotaxis. *Proc Natl Acad Sci USA* 103(5):1633–1638.
21. Smith RS, et al. (2006) A plausible model of phyllotaxis. *Proc Natl Acad Sci USA* 103(5):1301–1306.
22. Stoma S, et al. (2008) Flux-based transport enhancement as a plausible unifying mechanism for auxin transport in meristem development. *PLOS Comput Biol* 4(10):e1000207.
23. Nole-Wilson S, Tranby TL, Krizek BA (2005) AINTEGUMENTA-like (AIL) genes are expressed in young tissues and may specify meristematic or division-competent states. *Plant Mol Biol* 57(5):613–628.
24. Mayer KF, et al. (1998) Role of WUSCHEL in regulating stem cell fate in the Arabidopsis shoot meristem. *Cell* 95(6):805–815.
25. Long JA, Barton MK (1998) The development of apical embryonic pattern in Arabidopsis. *Development* 125(16):3027–3035.
26. Sawa S, Ito T, Shimura Y, Okada K (1999) FILAMENTOUS FLOWER controls the formation and development of arabidopsis inflorescences and floral meristems. *Plant Cell* 11(1):69–86.
27. de Reuille PB, et al. (2006) Computer simulations reveal properties of the cell-cell signaling network at the shoot apex in Arabidopsis. *Proc Natl Acad Sci USA* 103(5):1627–1632.
28. Vernoux T, et al. (2011) The auxin signalling network translates dynamic input into robust patterning at the shoot apex. *Mol Syst Biol* 7:508.
29. Brunoud G, et al. (2012) A novel sensor to map auxin response and distribution at high spatio-temporal resolution. *Nature* 482(7383):103–106.
30. Galinha C, et al. (2007) PLETHORA proteins as dose-dependent master regulators of Arabidopsis root development. *Nature* 449(7165):1053–1057.
31. Zhao Y, et al. (2001) A role for flavin monooxygenase-like enzymes in auxin biosynthesis. *Science* 291(5502):306–309.
32. Won C, et al. (2011) Conversion of tryptophan to indole-3-acetic acid by TRYPTOPHAN AMINOTRANSFERASES OF ARABIDOPSIS and YUCCAs in Arabidopsis. *Proc Natl Acad Sci USA* 108(45):18518–18523.
33. Heisler MG, et al. (2005) Patterns of auxin transport and gene expression during primordium development revealed by live imaging of the Arabidopsis inflorescence meristem. *Curr Biol* 15(21):1899–1911.
34. Ljung K, Bhalerao RP, Sandberg G (2001) Sites and homeostatic control of auxin biosynthesis in Arabidopsis during vegetative growth. *Plant J* 28(4):465–474.
35. Mirabet V, Besnard F, Vernoux T, Boudaoud A (2012) Noise and robustness in phyllotaxis. *PLOS Comput Biol* 8(2):e1002389.
36. Leyser HMO, Furner IJ (1992) Characterization of 3 shoot apical meristem mutants of *arabidopsis thaliana*. *Development* 116:397–403.
37. Giulini A, Wang J, Jackson D (2004) Control of phyllotaxy by the cytokinin-inducible response regulator homologue ABPHYL1. *Nature* 430(7003):1031–1034.
38. Jackson D, Hake S (1999) Control of phyllotaxy in maize by the abphyl1 gene. *Development* 126(2):315–323.
39. Lee BH, et al. (2009) Studies of aberrant phyllotaxy1 mutants of maize indicate complex interactions between auxin and cytokinin signaling in the shoot apical meristem. *Plant Physiol* 150(1):205–216.
40. Zhao Z, et al. (2010) Hormonal control of the shoot stem-cell niche. *Nature* 465(7301):1089–1092.
41. Hay A, Tsiantis M (2006) The genetic basis for differences in leaf form between Arabidopsis thaliana and its wild relative Cardamine hirsuta. *Nat Genet* 38(8):942–947.
42. Reddy GV, Meyerowitz EM (2005) Stem-cell homeostasis and growth dynamics can be uncoupled in the Arabidopsis shoot apex. *Science* 310(5748):663–667.
43. Gordon SP, et al. (2007) Pattern formation during de novo assembly of the Arabidopsis shoot meristem. *Development* 134(19):3539–3548.
44. Grandjean O, et al. (2004) In vivo analysis of cell division, cell growth, and differentiation at the shoot apical meristem in Arabidopsis. *Plant Cell* 16(1):74–87.